INVITED PAPER *Special Section on Distinguished Papers in Photonics*

Advanced Photonic Crystal Nanocavity Quantum Dot Lasers*

Yasutomo OTA[†a)], **Katsuyuki WATANABE**[†], **Masahiro KAKUDA**[†], ***Nonmembers***,
Satoshi IWAMOTO[†,††], ***Member***, ***and*** **Yasuhiko ARAKAWA**[†,††], ***Fellow***

SUMMARY We discuss our recent progress in photonic crystal nanocavity quantum dot lasers. We show how enhanced light matter interactions in the nanocavity lead to diverse and fascinating lasing phenomena that are in general inaccessible by conventional bulky semiconductor lasers. First, we demonstrate thresholdless lasing, in which any clear kink in the output laser curve does not appear. This is a result of near unity coupling of spontaneous emission into the lasing cavity mode, enabled by the strong Purcell effect supported in the nanocavity. Then, we discuss self-frequency conversion nanolasers, in which both near infrared lasing oscillation and nonlinear optical frequency conversion to visible light are simultaneously supported in the individual nanocavity. Owing to the tight optical confinement both in time and space, a high normalized conversion efficiency over a few hundred %/W is demonstrated. We also show that the intracavity nonlinear frequency conversion can be utilized to measure the statistics of the intracavity photons. These novel phenomena will be useful for developing various nano-optoelectronic devices with advanced functionalities.

key words: *photonic crystals, quantum dots, light matter interactions, nanolasers, nonlinear optics*

1. Introduction

Nanolasers have been of great interest due to their prospects for diverse applications. Their small footprints and energy consumption are highly desirable as light sources in future dense optical interconnects [1]. Their large surface to volume ratios make them sensitive to environmental change and thus are suitable for bio/chemical sensing [2]–[4]. So far, various nanolasers have been realized in many different optical platforms including photonic crystals (PhCs) [5]–[9], plasmonic materials [10]–[12] and nanowires [13]–[15]. Such nanocavities confine light tightly both in time and space. Among them, PhC nanocavities are in general superior in supporting high Q factors while keeping small mode volumes (Vs) close to the diffraction limit [16], which is roughly quantified as the cubic of half wavelength in the medium. Currently, the record-high Q factor for the telecom wavelength PhC nanocavities reaches eleven million [17], roughly corresponding to ∼10 ns cavity lifetime despite its wavelength scale size. With advanced PhC nanocavity design, it is also possible to achieve much smaller mode volumes far beyond the diffraction limit while keeping high Q factors [18]–[20].

The tight optical confinement in such nanocavities leads to the dramatic enhancement of light-matter interactions. A well-known consequence of this is the emergence of cavity quantum electrodynamics (cavity QED) effects [21], such as the Purcell effect for enhancing spontaneous emission rate into the cavity mode and the vacuum Rabi oscillation as a result of coherent energy exchange between the cavity photons and matter. These cavity QED effects are highly beneficial for boosting performances of nanolasers: indeed, the Purcell effect is known to be useful for increasing the differential gain for lasing [22]. Another prominent consequence of the enhanced light matter interactions is strong optical nonlinearity within the nanocavity [23], [24], which can be employed for further functionalizing the nanocavities and nanolasers [25]–[27]. For example, the intra-nanocavity nonlinear frequency conversion is expected to provide a novel route to synthesis arbitrary wavelength of light on ultra-compact platforms and to conduct quantum frequency conversion [28].

Nanolaser performances and functionalities are also largely affected by light emitters enclosed within the resonator. Among various gain media, gain properties of semiconductor quantum dots (QDs) [29] are known to be advantageous due to their high temperature stability, low linewidth enhancement factor and the resulting insensitivity against the feedback noise, and capability to suppress the nonradiative recombination. Moreover, QDs are also appropriate for studying cavity QED because of their atom like quantum emission in the solid state [30]–[33]. The use of QDs as a gain material will facilitate the development of nanolasers that can actively tailor the light matter interactions.

In this review article, we discuss PhC nanocavity QD lasers that have been recently developed in our group. The nanolasers possess distinguished properties and functionalities as a result of the enhanced light matter interactions. In the first half, we discuss thresholdless lasing using QDs [34], which has been achieved by efficiently funneling QD's spontaneous emission into a single PhC nanocavity mode by mainly using the Purcell effect. In the latter part, we discuss self-frequency conversion nanolasers [26], [27], [35], which generate coherent light at different wavelengths than those at the lasing peaks, via intra-nanocavity nonlinear frequency conversion of the internally-generated laser light.

Manuscript received October 31, 2017.
Manuscript revised January 17, 2018.
*This is a review article.
[†]The authors are with Nanoquine, The University of Tokyo, Tokyo, 153–8505 Japan.
[††]The authors are with IIS, The University of Tokyo, Tokyo, 153–8505 Japan.
a) E-mail: ota@iis.u-tokyo.ac.jp
DOI: 10.1587/transele.E101.C.553

2. Thresholdless QD Nanolaser

2.1 Spontaneous Emission Coupling Factor and Thresholdless Lasing

In general, an abrupt intensity increase occurs in a laser device when crossing its lasing threshold. This arises from device inefficiency below the laser threshold, meaning that injected energy into the system below threshold are predominantly wasted in the form of spontaneous emission into free space or non-radiative processes. The fraction of spontaneous emission that couples to the lasing cavity mode is quantified by spontaneous emission coupling factor, β. Larger β improves the device efficiency below the threshold and hence results in smaller intensity jump when surpassing the lasing threshold.

These laser behaviors are well described by the following laser rate equation for a single mode semiconductor laser [22], [36]:

$$\frac{dn}{dt} = -\kappa n + \beta\gamma(N - N_t)n + \beta\gamma N \tag{1}$$

$$\frac{dN}{dt} = P - (\gamma + \gamma_{nr})N - \beta\gamma(N - N_t)n, \tag{2}$$

where n is the cavity photon number, N is the carrier number, P is the carrier injection rate, κ is the cavity leakage rate, γ is the total spontaneous emission rate, γ_{nr} is the non-radiative recombination rate and N_t is the transparent carrier number. The threshold pump rate deduced from the above rate equations and a conventional threshold definition (gain is assumed to equal loss) is

$$\mathrm{P}_{th} = \frac{\kappa}{\beta}\left(1 + \frac{\gamma_{nr}}{\gamma}\right)\left(1 + \frac{\beta\gamma N_t}{\kappa}\right), \tag{3}$$

which suggests lower threshold with larger β. In the set of the rate equations, the term, $\beta\gamma(N - N_t)n$, describes the stimulated emission or absorption by the injected carriers. The differential gain, $\beta\gamma$, corresponds to spontaneous emission rate into the cavity mode (γ_c) and can be engineered by cavity QED effects. When using a high Q/V cavity, γ_c can be largely increased through the Purcell effect ($\propto Q/V$). β is equal to $\gamma_c/(\gamma_c + \gamma_{other})$, where γ_{other} is spontaneous emission rate into optical modes other than the lasing cavity mode. The photonic bandgap effect in PhCs suppresses spontaneous emission into free space [37], [38] and the small cavity sizes of PhC nanocavities enlarge free spectral range, both resulting in the reduction of γ_{other}. Overall, PhC nanocavities are in essence advantageous to largely increase β.

The amount of the "intensity jump" accompanied by lasing can be quantified by the change in the slope efficiency below and above the threshold. The ratio of the two slopes, J, is expressed as [34], [36]:

$$J = \beta^{-1}\left(1 + \frac{\gamma_{nr}}{\gamma} + \left(1 - \beta + \frac{\gamma_{nr}}{\gamma}\right)\frac{\beta\gamma N_t}{\kappa}\right). \tag{4}$$

If J is close to unity, the laser device will not exhibit any clear threshold behavior in the output curve. This behavior is called as thresholdless lasing and has been of great interest for nearly three decades [39], [40]. To achieve the thresholdless lasing or $J \sim 1$, it is vital to achieve (1) near unity β, (2) negligible γ_{nr} compared to γ and (3) weak absorption of intracavity photons by the gain material before the cavity leakage, which is quantified by $\beta\gamma N_t/\kappa$. The absorbed photons cannot be reconverted to the cavity photons with a probability of $1 - \beta + \gamma_{nr}/\gamma$. To these ends, well-engineered semiconductor QDs is one of the best choices as gain medium in particular due to its potential to the realization of high Purcell effect and its low non-radiative recombination rate.

Thresholdless lasing with $\beta \sim 1$ can be regarded as an ultimate form of lasers [40] in the sense that it utilizes the maximum possible differential gain ($\beta\gamma$) from a given spontaneous emission (γ). An outstanding advantage of a high $\beta\gamma$ is a wide intensity modulation bandwidth, which roughly coincides with the relaxation oscillation frequency $\omega_r/2\pi$ expressed as [41]

$$\omega_r^2 = \beta\gamma\kappa n_0\left(1 - \frac{1}{n_0}\frac{\beta\gamma N_t}{\kappa}\right) - \frac{1}{4}\left[\frac{\kappa + \beta\gamma N_t}{n_0 + 1} + \gamma\left(1 + \beta n_0 + \frac{\gamma_{nr}}{\gamma}\right)\right]^2, \tag{5}$$

where n_0 is the average intracavity photon number. This expression is derived through the small signal analysis of the above laser rate equations. For conventional lasers, the first term becomes the leading order, resulting in $\omega_r \sim \sqrt{\beta\gamma\kappa n_0}$, which indicates square root dependence of ω_r with β. Overall, thresholdless lasers are expected to operate as low threshold lasers with fast intensity modulation capability.

So far, there are several reports claiming the observation of thresholdless lasing [10], [42], [43]. Meanwhile, the validation of the thresholdless lasing is often not straightforward owing to the absence of clear threshold behavior in the output curve [44]. Therefore, it is essential to conduct comprehensive analyses on the laser properties from diverse points of view including output power, linewidth narrowing, second order coherence, relaxation oscillation and carrier life time. In particular, for confirming lasing, the manifestation of coherence of output light is indispensable, which should appear in changes in the first and second order coherence. In this context, there are so far no convincing experiment of thresholdless lasing, in particular for QD-based systems.

In the following, we discuss the realization of thresholdless lasing using QDs [34]. The thresholdless lasing is achieved in a GaAs-based two dimensional PhC nanocavity laser with InAs QD gain, as schematically shown in Fig. 1 (a). While this PhC QD nanolaser structure itself is the same as the conventional ones, we achieved its thresholdless operation by introducing cavity resonant excitation for optical carrier injection. The lasing oscillation is

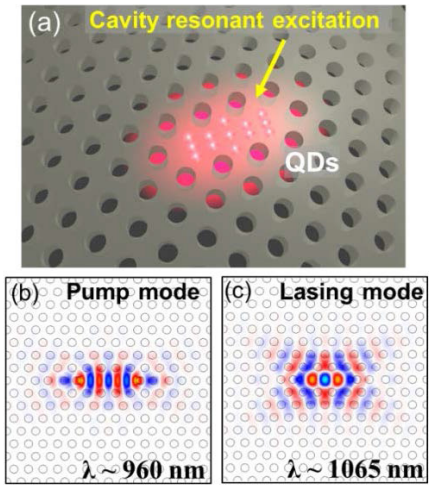

Fig. 1 (a) Schematic of the laser structure. Field distribution of (b) the pump and (c) lasing cavity mode. Adapted from [34].

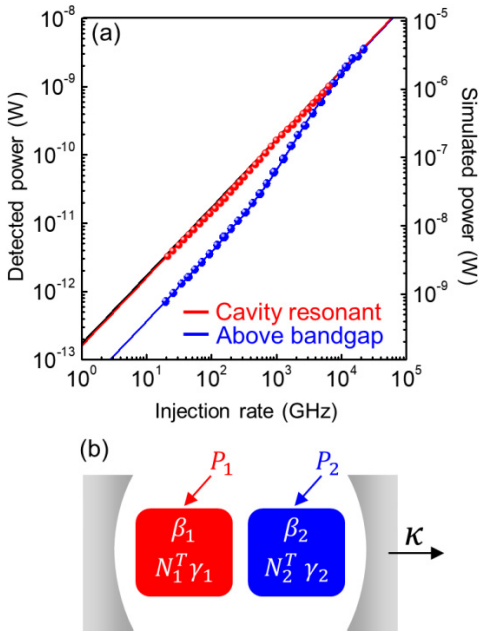

Fig. 2 (a) Measured LL curves. (b) Laser model with two carrier reservoirs. Adapted from [34].

carefully confirmed through measuring its output power, linewidth narrowing, second order coherence and so on.

2.2 Experimental Demonstration of Thresholdless Lasing

As discussed above, PhC nanocavities can support large Purcell effect together with the bandgap effect, the combination of which significantly increases β. Nevertheless, achievable βs in PhC nanocavity lasers are in general limited to on the order of 0.1. One of the causes of this non-unity β is the distribution of emitters in the exterior of the nanocavity, where cavity field strength reduces, and so does the Purcell effect. Therefore, the limited gain region within the high cavity field regions is required to achieve a very high β. For nanolasers with quantum well gain, this has been examined by using ultrasmall plasmonic cavity [10] and by PhC nanocavity with buried heterostructure active region [9], [42].

In the current work, we limit the QD active region by using cavity resonant excitation [45], [46], by which carriers are injected only within the center of the nanocavity (see Fig. 1 (a)). We used a tunable laser source to resonantly pump the fifth order cavity mode at 960 nm, the field profile of which is shown in Fig. 1 (b). Photon absorption selectively occurs within the high field regions of the mode, which have a large spatial overlap with the fundamental cavity mode resonating at 1065 nm (Fig. 1 (c)). The resonant wavelength of the fifth mode roughly coincides with the second excited states of the QDs, resulting in the direct injection of carriers into the QDs. The three dimensional confinement effect of the QDs traps the carriers and prevents their diffusion: the carriers simply relax to the ground states of the QDs and radiatively couple to the fundamental cavity mode with high βs. A beauty of this strategy is its convenience for the comparison with the conventional imperfect-β lasing, which is achievable in the same device simply by switching the pumping scheme to conventional above bandgap excitation with an 808 nm laser source. The pumping to the GaAs barrier matrix largely reduces the spatial selectivity in the carrier injection process and so does β. We performed relevant experiments using low temperature (15 K) micro photoluminescence measurement setup. The sample was mounted on a helium flow cryostat and its position was accurately controlled using a combination of stepping motor actuators and a two-axes piezo stage. The cavity resonant excitation is so sensitive to the relative position of the pump laser spot and the sample that it can be used to precisely re-position the sample during the experiments.

Figure 2 (a) shows logarithmic scale plots of light-in-light-out (LL) curves measured under the cavity resonant (red) and above bandgap (blue) excitation. For the above bandgap excitation, a s-shape curve with mild but clear kinks was observed, suggesting a conventional behavior of a PhC nanolaser with a moderately high β. Meanwhile, for the cavity resonant excitation, a highly straight LL curve was observed, suggesting its thresholdless behavior. In the plot, the detected powers in the vertical axis were deduced from peak areas extracted by fitting to the emission spectra and the lateral axis corresponds to the carrier injection rate, which is deduced from fitting the experimental LL curves to a semiconductor laser model. The model is based on the laser rate equation in Eqs. (1) and (2) but having two carrier reservoirs in order to express the QDs in the center (high β) and exterior (low β) of the cavity. A schematic of the model is shown in Fig. 2 (b). Here, we estimated $N_1{}^T$ to be 47, which can be read as the number of QDs in the carrier reservoir, after taking account into the presence of multiple excitonic states in the QD. The fitting curves are plotted as solid lines in Fig. 2 (a), exhibiting excellent agreements with the experimental curves. Deduced βs from the two fitting LL curves are 0.97 (thresholdless) and 0.22 (thresholded),

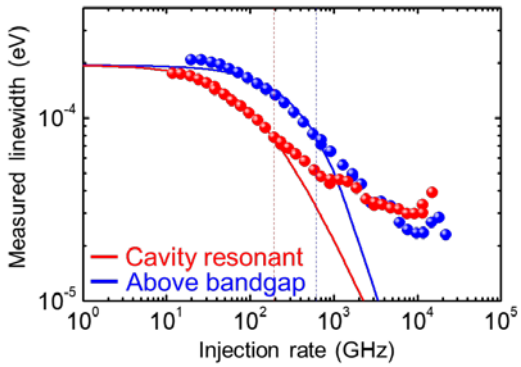

Fig. 3 Measured linewidths as a function of the injection rate. Adapted from [34].

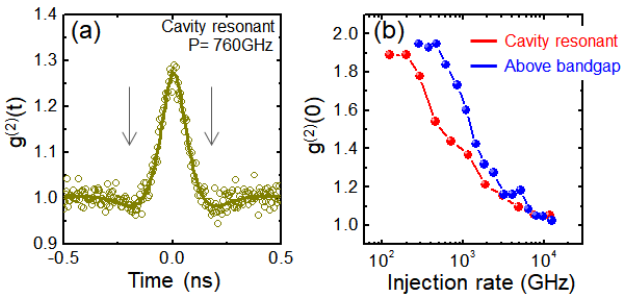

Fig. 4 (a) Measured $g^{(2)}(t)$ curve. (b) Evolutions of $g^{(2)}(0)$ as a function of injection rate. Adapted from [34].

respectively. It is noteworthy that the measured output powers can be well explained by the simulated power after the consideration of the detection efficiency of the optical setup (∼0.1%), which is limited by the coupling from the cavity to the objective lens and the throughput of the detection path.

Figure 3 shows evolutions of the linewidths as a function of carrier injection rate. For both the two excitation schemes, we observed significant linewidth narrowings by roughly one order of magnitude when increasing the injection rate. For low injection rates, the two linewidth curves are merged into a zero pump linewidth of about 200 μeV. We fitted the linewidth evolutions using a simple linewidth model [22] based on the laser model shown in Fig. 2 (b). The model curves well describe the observed linewidth evolutions for low injection rates. Meanwhile, discrepancies rapidly appear for larger pump rates after the points indicated by vertical dashed lines, at which positive gains emerge in the model and the resulting gain-refractive index coupling is expected to deviate the experimental linewidth behavior from that of the model. These results consistently suggest the development of the first order coherence in the device due to lasing.

We also investigated the evolution of the second order coherence by performing intensity correlation measurements with a Hanbury Brown-Twiss setup composed of a half beamsplitter and two ultrafast single photon counters. An example of the measured second order coherence curve, $g^{(2)}(t)$, is shown in Fig. 4 (a). The time, t, describes the delay between the timing of clicks of the two photon counters. The curves is measured under the cavity resonant excitation at an injection rate of 760 GHz, where the device is expected to be at the onset of lasing. $g^{(2)}(t)$ has a peak at the time zero. This peak originates from the fluctuation of the photon number within the nanocavity. The peak quickly decays with an oscillatory behavior, corresponding to self-noise driven relaxation oscillation [41], [47]. Since $g^{(2)}(t)$ is in essence a Fourier transform of relative intensity noise (RIN) spectrum, the oscillation frequency of ∼10 GHz of the $g^{(2)}(t)$ indicates the peak position in the RIN curve. Therefore, intensity modulation of ∼10 GHz could be possible despite the low simulated output power of ∼100 nW under this injection condition. Next, we summarize the pump power dependence of the peak height at the zero time delay, $g^{(2)}(0)$ in Fig. 4 (b). The $g^{(2)}(0)$ value corresponds to the relative photon intensity noise compared to coherent state in the nanocavity. For light in the thermal state, $g^{(2)}(0)$ is expected to be 2, while for in the coherent state, $g^{(2)}(0) = 1$. In the experimental results for both the pumping schemes, we observed transitions of $g^{(2)}(0)$ from thermal like ($g^{(2)}(0) \sim 2$) to coherent like ($g^{(2)}(0) \sim 1$) state as injection rate increases. This observation further supports the occurrence of lasing in our device. The faster transition of $g^{(2)}(0)$ for the thresholdless case could be due to faster accumulation of photons in the nanocavity (hence higher stimulated emission) owing to the higher β.

In summary, we demonstrate thresholdless lasing in a PhC QD nanolaser using the cavity resonant excitation. We clearly confirmed the lasing oscillation via comprehensive analyses on the laser output power, linewidth and $g^{(2)}(t)$. The observed thresholdless lasing was compared with the thresholded lasing realized in the same device driven under above bandgap excitation, which helps the understanding of the underlying physics in the thresholdless operation. Our work will be of importance for developing low power consumption nanolasers with fast intensity modulation capability.

3. Self-Frequency Conversion Nanolasers

3.1 Nonlinear Optics within Nanocavities

The tight optical confinement in nanocavities significantly enhances nonlinear interactions between intracavity photons, opening a pathway to develop ultra-compact nonlinear optical devices. For the second order nonlinear frequency conversion in nanocavity, the conversion efficiency normalized by the input power is inversely proportional to the square of V. The interaction length with the nonlinear optical medium can be effectively elongated by increasing Q. Overall, the conversion efficiency is proportional to $(Q/V)^2$. Another advantage of the use of the nanocavities is the lack of the strict requirement for phase matching between related optical modes. Tightly-confined nanocavity modes are composed of light with diverse wave vectors, mitigating the influence of phase mismatch between the propagating modes.

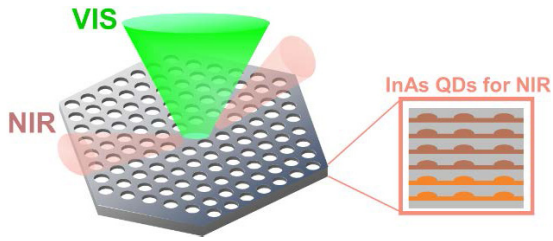

Fig. 5 Schematic of the self-frequency conversion nanolaser. Adapted from [26].

This corresponds to the fact that the conversion efficiency is predominantly determined by the spatial mode distributions of the related modes, which do not easily deform for the case of nanocavities. The lack of the strict phase matching requirement removes the need to precisely control the nanocavity environment, such as temperature. By taking advantages of these superiorities of the nanocavities, it could be possible to develop novel, ultra-compact, and simple-use nonlinear optical frequency mixers.

3.2 Nanocavity-Based Self-Frequency Conversion Lasers

Figure 5 shows the concept of in-situ nonlinear frequency conversion in nanocavity, in which we consider a GaAs-based PhC nanocavity. GaAs is a well-known material that possesses a high nonlinear optical susceptibility of 170pm/V in the near infrared (NIR). We introduce InAs QDs in the nanocavity, by which light can be internally generated through optical/electrical injection of carriers. We assume NIR lasing based on the QD gain and subsequent frequency conversion of the internally-generated cavity photons by nonlinear optical processes. As such, we can relieve the difficulty of introducing light from outside into nanoscale photonic structures. This system can be regarded as a self-frequency conversion nanolaser since the laser crystal supports both the lasing oscillation and nonlinear frequency conversion. In the following, we discuss self-frequency conversion nanolasers exhibiting second harmonic generation (SHG) for emitting visible (VIS) light. For experimental investigations, we again used the low temperature (10 K) micro photoluminescence measurement setup equipped with a continuous wave 808 nm pump laser source.

A typical optical output behavior of a self-frequency conversion nanolaser is shown in Fig. 6 (a), together with measured emission spectrum taken with a pump power of 42 μW (Fig. 6 (b)). For the NIR output, a conventional LL curve for a PhC QD nanolaser is observed with smooth kinks indicating its relatively-high β. The Q factor for the NIR lasing mode was measured to be 17,000. At the same time, the device exhibits VIS light output at the half wavelength of the NIR laser peak. The VIS output intensities quadratically increase compared with the NIR counterparts, suggesting that they originate from the intracavity SHG. From the two curves, we could deduce a high normalized frequency conversion efficiency of 13 %/W. After the

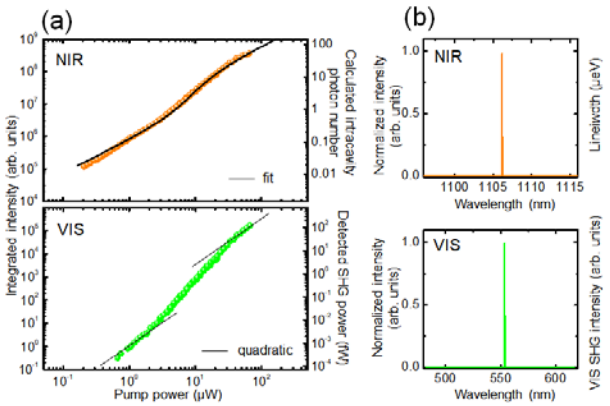

Fig. 6 Measured LL curves for the NIR (top) and VIS (bottom) peak. (b) Emission spectra measure with a pump power of 42 μW. Adapted from [27].

calibration of the detection efficiency of the optical setup, the conversion efficiency is estimated to be a few hundreds %/W. Thanks to this high efficiency, surprisingly, the VIS converted light was observable even below the lasing threshold around a pump power of 1 μW, where the estimated NIR intracavity photon number is only ~0.1 on average. The observation of this low photon number SHG suggests the possible use of the nanocavity for the study and applications of quantum few-photon nonlinear optics. It is worth emphasizing that the efficient frequency conversion is simply performed under the lack of careful control of temperature. In addition, we used uncomplicated non-resonant optical pumping aiming at carrier injection, rather than resonant optical excitation requiring finely tunable lasers for exciting the high Q cavity mode.

Leveraging the easiness of the device operation, together with the broad gain of the QD in the NIR, we demonstrate generation of diverse VIS light using multiple different PhC nanolasers with different resonant wavelengths. The nanolaser are integrated on a single semiconductor chip and are operated under a fixed temperature of 10 K. The pump power was chosen to either 1.5 or 3.0 mW. Figure 7 shows a series of measured color images of the different nanocavities with different PhC lattices constants ranging from 244 nm to 340 nm. Each device lases at a NIR wavelength spanning from 940 nm to 1260 nm, which is then doubled in frequency to generate the VIS light spanning from 470 nm (cyan) to 630 nm (red). The frequency conversion efficiency of each devices did not vary largely. This stable behavior can be understood as a result of the phase matching free operation of the self-frequency conversion lasers.

3.3 Quantum Phenomena in Nonlinear Optical Processes

The frequency conversion processes are in general affected by the quantum nature of photons [48]. For example, SHG is a process that combines two photons into one and thus cannot occur when there is only one photon in the field. In

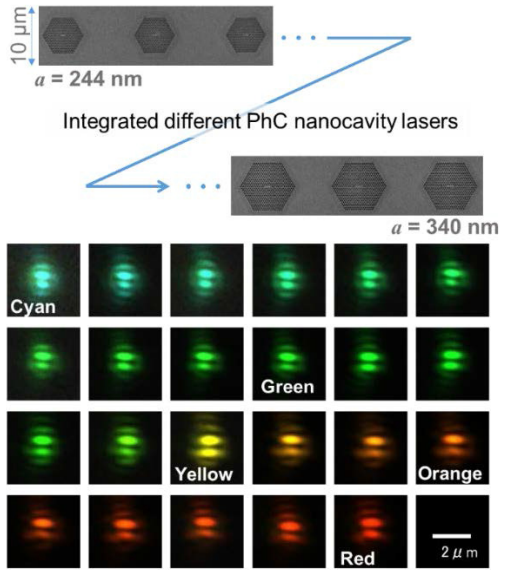

Fig. 7 VIS light emission from integrated multiple self-frequency conversion nanolasers. Adapted from [26].

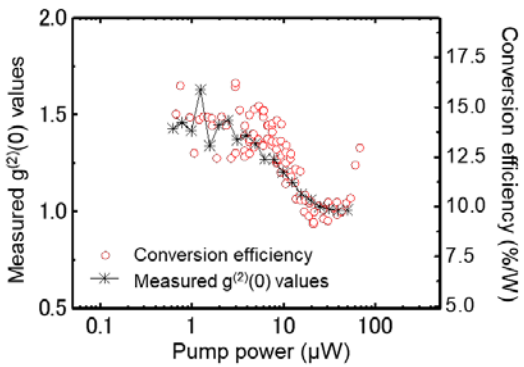

Fig. 8 Measured $g^{(2)}(0)$ values and normalized nonlinear frequency conversion efficiencies plotted as a function of pump power. Adapted from [27].

other words, the efficiencies of nonlinear optical processes reflect the photon statistics (photon number distribution) of the source field. Indeed, the normalized nonlinear frequency conversion efficiency of SHG process is known to be proportional to $g^{(2)}(0)$ [48], which is a measure of photon bunching (coalescence of multiple photons).

We examined such quantum nature of the nonlinear optical processes by measuring the SHG efficiency in a self-frequency conversion nanolaser [27]. We utilized the fact that the laser changes photon statistics ($g^{(2)}(0)$ value) from thermal like ($g^{(2)}(0) \sim 2$) to coherent like ($g^{(2)}(0) \sim 1$) when crossing the laser threshold, as discussed in the previous section. For measuring $g^{(2)}(0)$, we again employed the Hanbury Brown-Twiss measurement setup. Figure 8 shows measured evolutions of $g^{(2)}(0)$ and the normalized nonlinear frequency conversion efficiencies as a function of the pump power. Regarding $g^{(2)}(0)$, we observed a transition from thermal like ($g^{(2)}(0) \sim 1.5$) to coherent like ($g^{(2)}(0) \sim 1$) state when surpassing the threshold pump power of ~8 μW. Meanwhile, the conversion efficiencies show a similar transition and change the efficiency from ~15%/w to ~10%/W across the threshold. The two overlaid curves are well comparable each other, suggesting the proportionality of the conversion efficiency to $g^{(2)}(0)$, as expected from a quantum theory of the intracavity SHG process [27]. It is noteworthy that the conversion process occurs within the Heisenberg time, which is the Planck constant divided by the photon energy and is about a few fs in this case. These results suggest that the intra-nanocavity SHG can be used for ultrafast sensing of the photon statistics in very compact devices and could provide a fascinating platform to explore novel quantum applications.

4. Conclusion

In this review, we discuss our recent efforts for advancing PhC QD nanolasers. We have demonstrated thresholdless lasing in a QD device and nanocavity-based self-frequency conversion lasers. Both the lasing phenomena are consequences of enhanced light matter interactions due to the tight optical confinement in the nanocavity. For both devices, the next important step is to demonstrate the functionalities at room temperature under electrical carrier injection. To this end, it would be essential to employ buried heterostructure for QD active regions [9], together with the development of QDs with very low inhomogeneous spectral broadening. In addition, it will be essential to clarify the influence of the Purcell effect at room temperature, at which strong dephasing could significantly disturb the emergence of cavity QED effects. Further investigations are awaited for clarifying such complicated physics and for exploring novel devices useful for diverse applications.

Acknowledgments

The authors thank S. Ishida, M. Nishioka, N. Kumagai, K. Kamide, C.F. Fong, K. Kuruma and D. Takamiya for their technical support and for fruitful discussions. This works was supported by Project for Developing Innovation Systems of MEXT, JSPS KAKENHI Grant-in-Aid for Specially promoted Research (15H05700) and KAKENHI (16K06294) and is based on results obtained from a project commissioned by the New Energy and Industrial Technology Development Organization (NEDO).

References

[1] D.A.B. Miller, "Attojoule Optoelectronics for Low-Energy Information Processing and Communications," J. Light. Technol., vol.35, no.3, pp.346–396, 2017.
[2] S. Hachuda, T. Watanabe, D. Takahashi, and T. Baba, "Sensitive and selective detection of prostate-specific antigen using a photonic crystal nanolaser," Opt. Express, vol.24, p.12886, 2016.
[3] G. Shambat, S.-R. Kothapalli, J. Provine, T. Sarmiento, J. Harris, S.S. Gambhir, and J. Vučković, "Single-cell photonic nanocavity probes," Nano Lett., vol.13, no.11, pp.4999–5005, 2013.
[4] M. Lončar, A. Scherer, and Y. Qiu, "Photonic crystal laser

sources for chemical detection," Appl. Phys. Lett., vol.82, no.26, pp.4648–4650, 2003.
[5] O. Painter, R. Lee, A. Scherer, A. Yariv, J. O'Brien, P. Dapkus, and I. Kim, "Two-dimensional photonic band-Gap defect mode laser," Science, vol.284, pp.1819–21, 1999.
[6] T. Yoshie, O.B. Shchekin, H. Chen, D.G. Deppe, and A. Scherer, "Quantum dot photonic crystal lasers," Electron. Lett., vol.38, no.17, pp.967–968, 2002.
[7] M. Nomura, S. Iwamoto, K. Watanabe, N. Kumagai, Y. Nakata, S. Ishida, and Y. Arakawa, "Room temperature continuous-wave lasing in photonic crystal nanocavity," Opt. Express, vol.14, no.13, pp.6308–6315, 2006.
[8] K. Nozaki, S. Kita, and T. Baba, "Room temperature continuous wave operation and controlled spontaneous emission in ultrasmall photonic crystal nanolaser," Opt. Express, vol.15, no.12, pp.7506–7514, 2007.
[9] S. Matsuo, A. Shinya, T. Kakitsuka, K. Nozaki, T. Segawa, T. Sato, Y. Kawaguchi, and M. Notomi, "High-speed ultracompact buried heterostructure photonic-crystal laser with 13 fJ of energy consumed per bit transmitted," Nat. Photonics, vol.4, no.9, pp.648–654, 2010.
[10] M. Khajavikhan, A. Simic, M. Katz, J.H. Lee, B. Slutsky, A. Mizrahi, V. Lomakin, and Y. Fainman, "Thresholdless nanoscale coaxial lasers," Nature, vol.482, no.7384, pp.204–207, 2012.
[11] M.T. Hill, Y.-S. Oei, B. Smalbrugge, Y. Zhu, T. de Vries, P.J. van Veldhoven, F.W.M. van Otten, T.J. Eijkemans, J.P. Turkiewicz, H. de Waardt, E.J. Geluk, S.-H. Kwon, Y.-H. Lee, R. Nötzel, and M.K. Smit, "Lasing in metallic-coated nanocavities," Nat. Photonics, vol.1, no.10, pp.589–594, 2007.
[12] R.F. Oulton, V.J. Sorger, T. Zentgraf, R.-M. Ma, C. Gladden, L. Dai, G. Bartal, and X. Zhang, "Plasmon lasers at deep subwavelength scale," Nature, vol.461, no.7264, pp.629–632, 2009.
[13] J. Tatebayashi, S. Kako, J. Ho, Y. Ota, S. Iwamoto, and Y. Arakawa, "Room-temperature lasing in a single nanowire with quantum dots," Nat. Photonics, vol.9, no.8, pp.501–505, 2015.
[14] D. Saxena, S. Mokkapati, P. Parkinson, N. Jiang, Q. Gao, H.H. Tan, and C. Jagadish, "Optically pumped room-temperature GaAs nanowire lasers," Nat. Photonics, vol.7, no.12, pp.963–968, 2013.
[15] B. Mayer, D. Rudolph, J. Schnell, S. Morkötter, J. Winnerl, J. Treu, K. Müller, G. Bracher, G. Abstreiter, G. Koblmüller, and J.J. Finley, "Lasing from individual GaAs-AlGaAs core-shell nanowires up to room temperature," Nat. Commun., vol.4, p.2931, 2013.
[16] Y. Akahane, T. Asano, B.-S. Song, and S. Noda, "High-Q photonic nanocavity in a two-dimensional photonic crystal," Nature, vol.425, no.6961, pp.944–947, 2003.
[17] T. Asano, Y. Ochi, Y. Takahashi, K. Kishimoto, and S. Noda, "Photonic crystal nanocavity with a Q factor exceeding eleven million," Opt. Express, vol.25, no.3, p.1769, 2017.
[18] H. Choi, M. Heuck, and D. Englund, "Self-Similar Nanocavity Design with Ultrasmall Mode Volume for Single-Photon Nonlinearities," Phys. Rev. Lett., vol.118, no.22, p.223605, 2017.
[19] S. Hu and S.M. Weiss, "Design of Photonic Crystal Cavities for Extreme Light Concentration," ACS Photonics, vol.3, no.9, pp.1647–1653, 2016.
[20] J.T. Robinson, C. Manolatou, L. Chen, and M. Lipson, "Ultrasmall Mode Volumes in Dielectric Optical Microcavities," Phys. Rev. Lett., vol.95, no.14, p.143901, 2005.
[21] P.R. Berman, *Cavity Quantum Electrodynamics*, Academic Press, 1994.
[22] G. Bjork and Y. Yamamoto, "Analysis of semiconductor microcavity lasers using rate equations," IEEE J. Quantum Electron., vol.27, no.11, pp.2386–2396, 1991.
[23] K. Rivoire, Z. Lin, F. Hatami, W.T. Masselink, and J. Vučković, "Second harmonic generation in gallium phosphide photonic crystal nanocavities with ultralow continuous wave pump power," Opt. Express, vol.17, no.25, pp.22609–22615, 2009.
[24] M.W. McCutcheon, J.F. Young, G.W. Rieger, D. Dalacu, S. Frédérick, P.J. Poole, and R.L. Williams, "Experimental demonstration of second-order processes in photonic crystal microcavities at submilliwatt excitation powers," Phys. Rev. B, vol.76, no.24, p.245104, 2007.
[25] K. Nozaki, A. Shinya, S. Matsuo, Y. Suzaki, T. Segawa, T. Sato, Y. Kawaguchi, R. Takahashi, and M. Notomi, "Ultralow-power all-optical RAM based on nanocavities," Nat. Photonics, vol.6, no.4, pp.248–252, 2012.
[26] Y. Ota, K. Watanabe, S. Iwamoto, and Y. Arakawa, "Nanocavity-based self-frequency conversion laser," Opt. Express, vol.21, no.17, p.19778, 2013.
[27] Y. Ota, K. Watanabe, S. Iwamoto, and Y. Arakawa, "Measuring the second-order coherence of a nanolaser by intracavity frequency doubling," Phys. Rev. A, vol.89, no.2, p.23824, 2014.
[28] M.W. McCutcheon, D.E. Chang, Y. Zhang, M.D. Lukin, and M. Loncar, "Broadband frequency conversion and shaping of single photons emitted from a nonlinear cavity," Opt. Express, vol.17, no.25, p.22689, 2009.
[29] Y. Arakawa and H. Sakaki, "Multidimensional quantum well laser and temperature dependence of its threshold current," Appl. Phys. Lett., vol.4, no.11, p.939, 1982.
[30] T. Yoshie, A. Scherer, J. Hendrickson, G. Khitrova, H.M. Gibbs, G. Rupper, C. Ell, O.B. Shchekin, and D.G. Deppe, "Vacuum Rabi splitting with a single quantum dot in a photonic crystal nanocavity," Nature, vol.432, no.7014, pp.200–203, 2004.
[31] J.P. Reithmaier, G. Sęk, A. Löffler, C. Hofmann, S. Kuhn, S. Reitzenstein, L.V. Keldysh, V.D. Kulakovskii, T.L. Reinecke, and A. Forchel, "Strong coupling in a single quantum dot-semiconductor microcavity system," Nature, vol.432, no.7014, pp.197–200, 2004.
[32] J. Gérard, B. Sermage, B. Gayral, B. Legrand, E. Costard, and V. Thierry-Mieg, "Enhanced Spontaneous Emission by Quantum Boxes in a Monolithic Optical Microcavity," Phys. Rev. Lett., vol.81, no.5, pp.1110–1113, 1998.
[33] Y. Arakawa, S. Iwamoto, M. Nomura, A. Tandaechanurat, and Y. Ota, "Cavity Quantum Electrodynamics and Lasing Oscillation in Single Quantum Dot-Photonic Crystal Nanocavity Coupled Systems," IEEE J. Sel. Topics Quantum Electron., vol.18, no.6, pp.1818–1829, 2012.
[34] Y. Ota, M. Kakuda, K. Watanabe, S. Iwamoto, and Y. Arakawa, "Thresholdless quantum dot nanolaser," Opt. Express, vol.25, no.17, p.19981, 2017.
[35] Y. Ota, K. Watanabe, S. Iwamoto, and Y. Arakawa, "Self-frequency summing in quantum dot photonic crystal nanocavity lasers," Appl. Phys. Lett., vol.103, no.24, p.243115, 2013.
[36] G. Björk, A. Karlsson, and Y. Yamamoto, "Definition of a laser threshold," Phys. Rev. A, vol.50, no.2, pp.1675–1680, 1994.
[37] M. Fujita, S. Takahashi, Y. Tanaka, and S. Noda, "Simultaneous Inhibition and Redistribution of Spontaneous Light Emission in Photonic Crystals," Science, vol.308, pp.1296–1298, 2005.
[38] M. Takiguchi, H. Sumikura, M. Danang Birowosuto, E. Kuramochi, T. Sato, K. Takeda, S. Matsuo, and M. Notomi, "Enhanced and suppressed spontaneous emission from a buried heterostructure photonic crystal cavity," Appl. Phys. Lett., vol.103, p.91113, 2013.
[39] H. Yokoyama, "Physics and device applications of optical microcavities," Science, vol.256, no.5053, pp.66–70, 1992.
[40] S. Noda, "Seeking the Ultimate Nanolaser," Science, vol.314, no.5797, pp.260–261, 2006.
[41] N. Takemura, J. Omachi, and M. Kuwata-Gonokami, "Fast periodic modulations in the photon correlation of single-mode vertical-cavity surface-emitting lasers," Phys. Rev. A, vol.85, no.5, p.53811, 2012.
[42] M. Takiguchi, H. Taniyama, H. Sumikura, M.D. Birowosuto, E. Kuramochi, A. Shinya, T. Sato, K. Takeda, S. Matsuo, and M. Notomi, "Systematic study of thresholdless oscillation in high-β buried multiple-quantum-well photonic crystal nanocavity lasers," Opt. Express, vol.24, no.4, p.3441, 2016.
[43] I.P. Rieto, J.M.L. Lorens, L.E.M.U. Amúñez, A.G.T. Aboada, J.C.A. Errer, J.M.R. Ipalda, C.R. Obles, G.M.U. Atutano, J.P.M.A. Astor, and P.A.P. Ostigo, "Near thresholdless laser operation at room tem-

perature," Optica, vol.2, pp.66–69, 2015.
[44] C.Z. Ning, "What is Laser Threshold?," IEEE J. Sel. Topics Quantum Electron., vol.19, no.4, p.1503604, 2013.
[45] M. Nomura, S. Iwamoto, M. Nishioka, S. Ishida, and Y. Arakawa, "Highly efficient optical pumping of photonic crystal nanocavity lasers using cavity resonant excitation," Appl. Phys. Lett., vol.89, no.16, p.161111, 2006.
[46] Y. Ota, M. Nomura, N. Kumagai, K. Watanabe, S. Ishida, S. Iwamoto, and Y. Arakawa, "Enhanced photon emission and absorption of single quantum dot in resonance with two modes in photonic crystal nanocavity," Appl. Phys. Lett., vol.93, no.18, p.183114, 2008.
[47] J. Wiersig, C. Gies, F. Jahnke, M. Assmann, T. Berstermann, M. Bayer, C. Kistner, S. Reitzenstein, C. Schneider, S. Höfling, A. Forchel, C. Kruse, J. Kalden, and D. Hommel, "Direct observation of correlations between individual photon emission events of a microcavity laser," Nature, vol.460, no.7252, pp.245–249, 2009.
[48] Y. Qu and S. Singh, "Photon correlation effects in second harmonic generation," Opt. Commun., vol.90, no.1-3, pp.111–114, 1992.

Yasutomo Ota received a B.E. (2006) in Mechanical Engineering from Osaka Prefecture University and a M.E (2008) and a Ph.D. (2011) in Electrical Engineering from The University of Tokyo. He joined Institute for Nano Quantum Information Electronics, University of Tokyo as a project assistant professor in 2011 and has been a project associate professor since 2016. His research interest lies in light-matter interactions in photonic nanostructures.

Katsuyuki Watanabe received his PhD from the Tokyo University of Science in 2001. He is a project research associate of the Institute for Nano Quantum Information Electronics at the University of Tokyo. His research interests include epitaxial growth, molecular beam epitaxy, and quantum-dot-based devices.

Masahiro Kakuda received a B.E in Applied Physics, a M.E. and a Ph.D. in Advanced Materials Science from The University of Tokyo in 2007, 2009, 2013, respectively. He joined Institute for Nano Quantum Information Electronics, The University of Tokyo as a project assistant professor in 2013. His research interest is the crystal growth and the applications of III-V semiconductor quantum dots.

Satoshi Iwamoto received the B.E., M.E., and Ph.D. degrees in applied physics from The University of Tokyo, Tokyo, Japan, in 1997, 1999, 2002, respectively. In 2002, he joined the Institute of Industrial Science, the University of Tokyo, as a Research Associate, and started research on photonic nanostructures. He was promoted to a Lecturer and an Associate Professor in 2003 and 2007. He received Young Scientist Presentation Award from JSAP (2000), SSDM Paper Award (2005), and Young Scientists' Prize from MEXT, Japan in 2012.

Yasuhiko Arakawa received his B.S., M.S., and Ph. D. degrees in Electrical. Eng. in 1975, 1977 and 1980, respectively, from the University of Tokyo. He has been a Full Professor of the University of Tokyo since 1993. He is now a Professor of Institute of Industrial Science and also the Director of Institute for Nano Quantum Information Electronics, both at the University of Tokyo. He received several distinguished awards, including Leo Esaki Prize, Fujiwara Prize, Prime Minister Award, I IEEE David Sarnoff Award, Medal with Purple Ribbon, C&C Award, Heinrich Welker Award, OSA Nick Holonyak Jr. Award, and Japan Academy Prize. He is a Foreign Member of US National Academy of Engineering.